

Q3

(a) The driving-point displacement FRF may be expressed as a modal sum:

$$H(x, y, \omega) = \sum_n \frac{u_n(x)u_n(y)}{\omega_n^2 + 2i\omega\omega_n\zeta_n - \omega^2} = \sum_n \frac{(u_n(x))^2}{\omega_n^2 + 2i\omega\omega_n\zeta_n - \omega^2}$$

At the fundamental resonance, this approximates to

$$H(\omega) \approx \frac{(u_1(x))^2}{2i\omega_1^2\zeta_1}$$

At low frequencies, this approximates to

$$H(\omega) \approx \sum_n \frac{(u_n(x))^2}{\omega_n^2} \approx \frac{(u_1(x))^2}{\omega_1^2}$$

Hence, the ratio of the amplitude at resonance to the pseudo-static response level gives

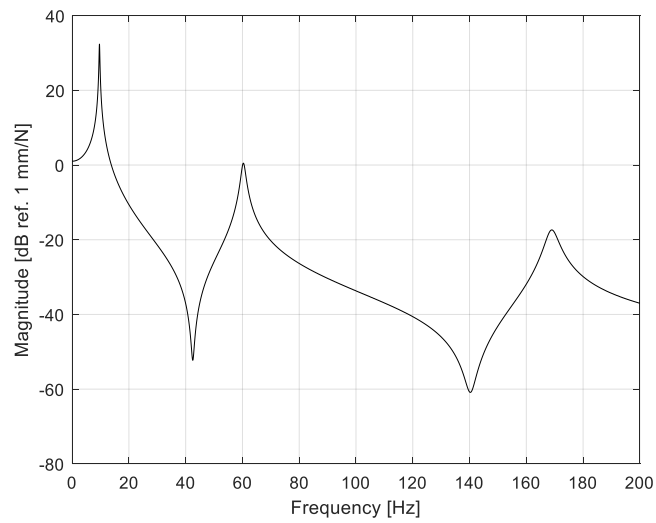
$$\frac{(u_1(x))^2}{2\omega_1^2\zeta_1} \frac{\omega_1^2}{(u_1(x))^2} = \frac{1}{2\zeta_1} = Q_1$$

Using the data in Table 1 gives $Q_1 = 41.56 / 1.13 = 37$

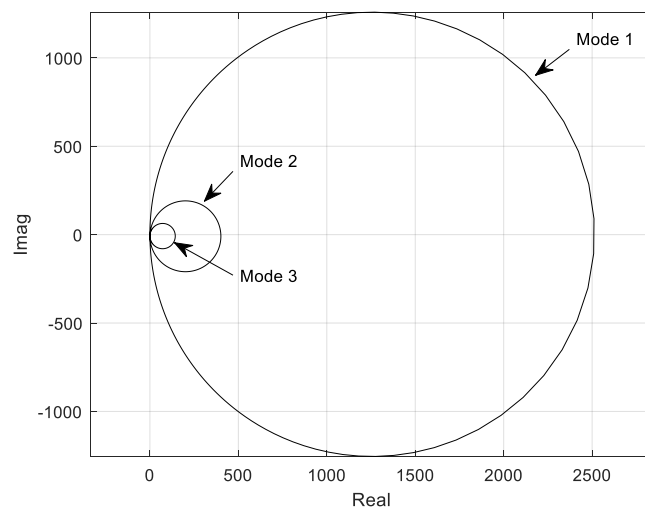
The half-power bandwidths are then calculated as f_n / Q_1 , assuming the Q-factor remains constant.

Mode	Frequency (Hz)	Response amplitude		Half-power bandwidth (Hz)	Velocity amplitude (mm/s/N)
		(mm/N)	(dB re mm/N)		
-	0.1	1.13	1.06	-	-
1	9.6	41.56	32.4	0.26	2507
2	60.3	1.06	0.51	1.63	402
3	168.9	0.14	-17.1	4.56	149

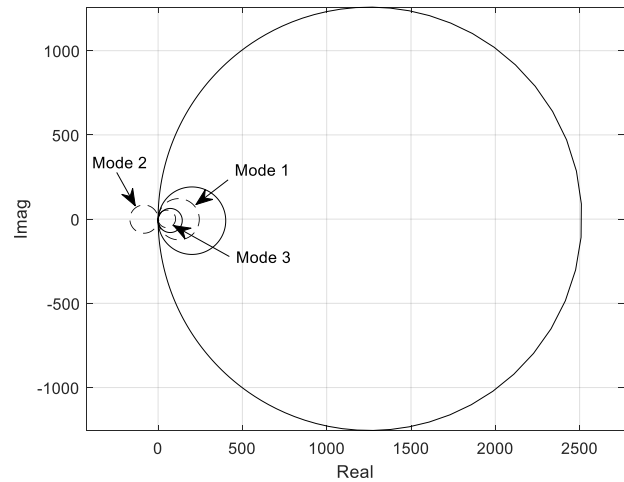
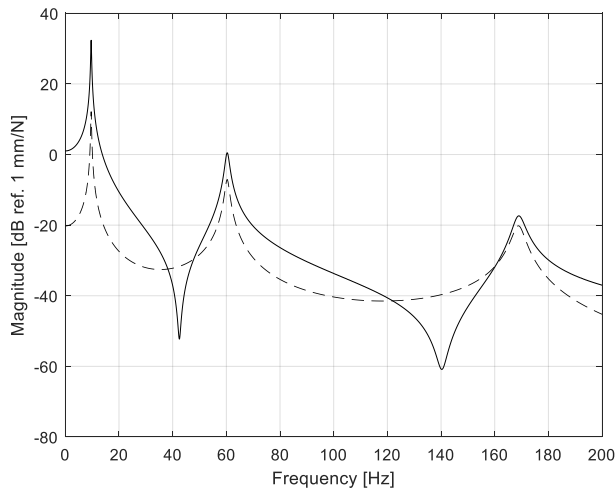
(b) Full marks for sketching the FRF are obtained by using correctly labelled axes and accounting for: the pseudo-static response; the level and frequency of each peak; the varying half-power bandwidths; and the presence of anti-resonances between the peaks (because this is a driving-point response).



(c) Full marks for sketching the velocity modal circles are obtained by calculating the circle diameters (angular frequency \times peak displacement amplitude – see final column of table) and correctly orientating the circles on the real axis.



(d) Moving the shaker close to the root reduces the response magnitude across all frequencies (although this is less significant at higher frequencies due to the changing positions of nodes/antinodes). All three modes are still evident, with the natural frequencies and modal bandwidths unchanged, but antiresonances are no longer present because this is now a transfer function. The modal circles are reduced in diameter; those for Mode 1 and 3 remain on the positive real axis but the Mode 2 circle is now on the negative real axis, which is deduced from considering the sign of the modal factor $u_n(x) u_n(y)$ at each resonance.



(e) In this application, the primary advantage of a hammer is its portability and ease of use (it also applies a purely normal force but this is less of an issue for the floor beam, which is axially stiff). The primary disadvantage is that it may not provide sufficient excitation for the heavily damped beam (Q -factor = 37), with the possibility of a poor signal/noise ratio, although repeated impacts and averaging would help mitigate this.

Q1

$$(a) \quad T = \frac{1}{2} m \sum \dot{y}_i^2$$

$$V = \frac{1}{2} k y_1^2 + \frac{1}{2} k (y_2 - y_1)^2 + \frac{1}{2} k (y_3 - y_2)^2$$

$$\text{so } M = m \begin{bmatrix} 1 & 0 & 0 \\ 0 & 1 & 0 \\ 0 & 0 & 1 \end{bmatrix}$$

$$K = k \begin{bmatrix} 2 & -1 & 0 \\ -1 & 2 & -1 \\ 0 & -1 & 1 \end{bmatrix}$$

$$k \begin{bmatrix} 2 & -1 & 0 \\ -1 & 2 & -1 \\ 0 & -1 & 1 \end{bmatrix} \begin{bmatrix} y_1 \\ y_2 \\ y_3 \end{bmatrix} = \omega^2 m \begin{bmatrix} 1 & & \\ & 1 & \\ & & 1 \end{bmatrix} \begin{bmatrix} y_1 \\ y_2 \\ y_3 \end{bmatrix}$$

$$k(2 - y_2) = \omega^2 m \quad \text{--- (1)}$$

$$k(-1 + 2y_2 - y_3) = \omega^2 m y_2 \quad \text{--- (2)}$$

$$k(-y_2 + y_3) = \omega^2 m y_3 \quad \text{--- (3)}$$

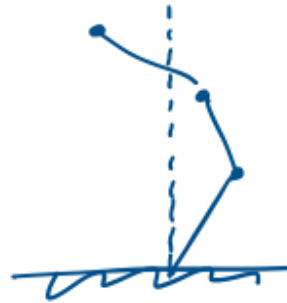
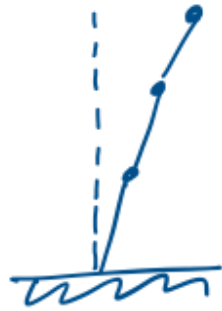
$$(1) \Rightarrow y_2 = 2 - \frac{\omega^2 m}{k}$$

$$(3) \Rightarrow y_3(\omega^2 m - k) = -ky_2$$

$$y_3 = \frac{ky_2}{(k - \omega^2 m)} = \frac{y_2}{\left(1 - \frac{\omega^2 m}{k}\right)}$$

$\omega^2 m/k$	y_1	y_2	y_3
0.1981	1	1.802	2.247
1.5550	1	0.445	-0.802
3.2470	1	-1.247	0.555

mode shapes: $\begin{bmatrix} 1 \\ 1.802 \\ 2.247 \end{bmatrix}$, $\begin{bmatrix} 1 \\ 0.445 \\ -0.802 \end{bmatrix}$, $\begin{bmatrix} 1 \\ -1.247 \\ 0.555 \end{bmatrix}$



(b) Four possibilities (others accepted if well justified):

- Boundary damping: microslip at joints
soil-structure interaction
- Fluid-structure interaction: viscous losses of air flowing around building.
- Fluid structure interaction: air pumping at interfaces.
- Material damping: not significant from steel, but floors/ceilings & other cladding/attachments.

(c) Power dissipated, $P = c \cdot (\dot{y}_2 - \dot{y}_1)^2$

Rayleigh's dissipation function, $R = \frac{1}{2} P = \frac{1}{2} c (\dot{y}_2 - \dot{y}_1)^2$

giving: $C = c \begin{bmatrix} 1 & -1 & 0 \\ -1 & 1 & 0 \\ 0 & 0 & 0 \end{bmatrix}$

(d) $M\ddot{y} + C\dot{y} + Ky = 0$

let $z = \begin{bmatrix} y \\ \dot{y} \end{bmatrix}$

$$A = \begin{bmatrix} 0 & I \\ -M^{-1}K & -M^{-1}C \end{bmatrix}$$

$$A = \begin{pmatrix} 0 & 0 & 0 & 1 & 0 & 0 \\ 0 & 0 & 0 & 0 & 1 & 0 \\ 0 & 0 & 0 & 0 & 0 & 1 \\ -2k/m & k/m & 0 & -c/m & c/m & 0 \\ k/m & -2k/m & k/m & c/m & -c/m & 0 \\ 0 & k/m & -k/m & 0 & 0 & 0 \end{pmatrix}$$

$$z = \begin{pmatrix} y_1 \\ y_2 \\ y_3 \\ \dot{y}_1 \\ \dot{y}_2 \\ \dot{y}_3 \end{pmatrix}$$

(c) (i) length 6 as z stacks displacement & velocity.
 ie for evec $\phi_n = \begin{pmatrix} u_n \\ \dot{u}_n \end{pmatrix} \rightarrow$ displacement 3×1
 \rightarrow velocity 3×1 .

(ii) • complex modes \Rightarrow magnitude & phase.

• displacements at different points in structure no longer reach max/min at same time.

• mode shapes appear to look a bit more like waves.

(iii) 6 total. Missing ones are conjugate pairs of pinked ones.

(iv) Note: $\lambda_n = -\sigma_n + i\omega_n$

$$\text{free response: } e^{\lambda_n t} = e^{-\sigma_n t} \cdot e^{i\omega_n t}$$

$\underbrace{\hspace{1.5cm}}_{\parallel}$
 $e^{-i\sigma_n t}$

$$\text{so } \zeta_n = \sigma_n / \omega_n, \quad \& \quad Q = \frac{\omega_n}{2\sigma_n}$$

$\operatorname{re}(\omega_n)$ $\operatorname{im}(\omega_n)$ ϕ_n Q

4.45

0.035

$$\begin{bmatrix} 1 \\ 1.8 \\ 2.25 \end{bmatrix}$$

64.4

12.48

0.083

$$\begin{bmatrix} 1 \\ 0.45 \\ -0.81 \end{bmatrix}$$

75.5

17.98

0.88

$$\begin{bmatrix} 1 \\ -1.2 \\ 0.54 \end{bmatrix}$$

10.2

(v) If damper between each floor then :

$$C = c \begin{bmatrix} 2 & -1 & 0 \\ 0 & 2 & -1 \\ 0 & -1 & 1 \end{bmatrix} \propto K$$

So now the structure is proportionally damped (ie example of Rayleigh damping $C = \alpha K + \beta M$).

Mode shapes will be real-valued, & overall damping will also be higher.

Q2

(a) $y = R F e^{i\omega t}$

PDE: $P \left(R'''' F + \frac{1}{r} R' F + \frac{1}{r^2} R F'' \right) = -\rho \omega^2 R F$

$\div R F P \Rightarrow \frac{R''''}{R} + \frac{1}{r} \frac{R'}{R} + \frac{1}{r^2} \frac{F''}{F} = -\frac{\rho \omega^2}{P}$

$\times r^2 \Rightarrow r^2 \frac{R''''}{R} + r \frac{R'}{R} + \frac{\rho \omega^2 r^2}{P} + \frac{F''}{F} = 0.$

$$SD: \quad \Gamma^2 \frac{R''}{R} + \Gamma \frac{R'}{R} + \frac{\rho \omega^2 r^2}{\rho} = -\frac{F''}{F} = \text{constant} = \nu^2$$

$$\textcircled{R}: \quad \Gamma^2 \frac{R''}{R} + \Gamma \frac{R'}{R} + \frac{\rho \omega^2 r^2}{\rho} = \nu^2$$

$$\textcircled{F}: \quad F'' + \nu^2 F = 0$$

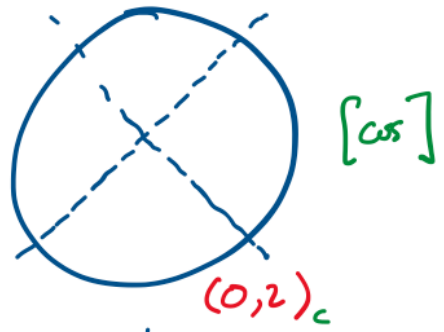
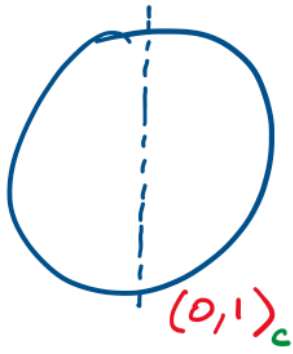
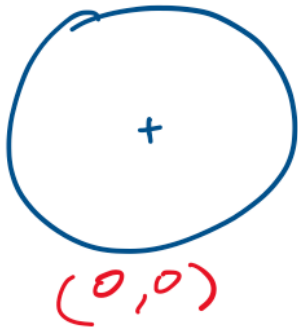
(b)

$n=0$

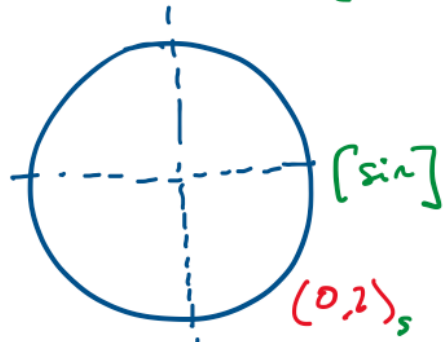
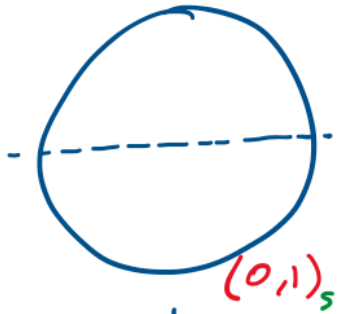
1

2

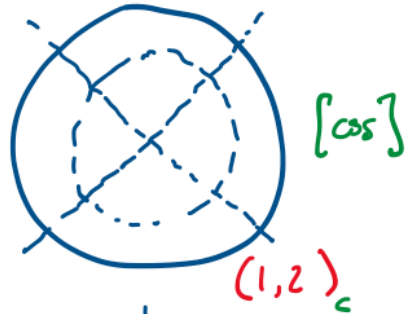
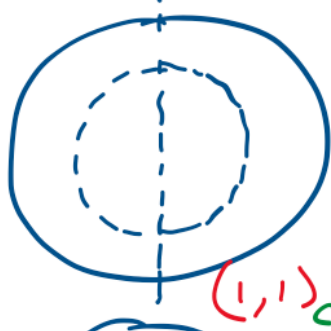
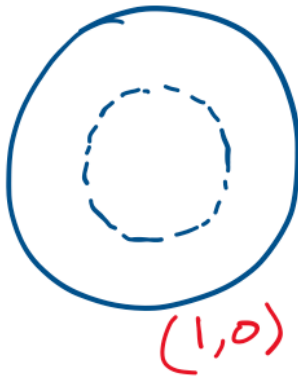
$m=0$



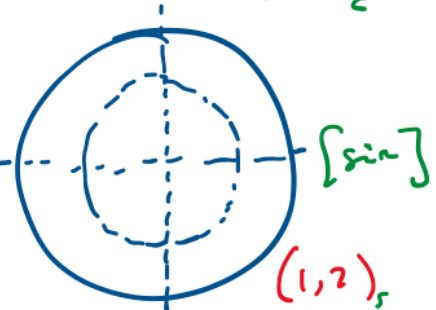
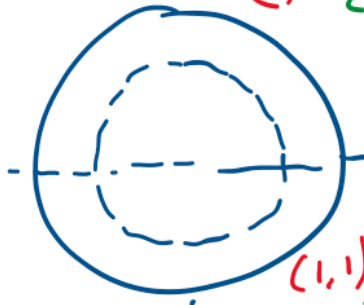
0



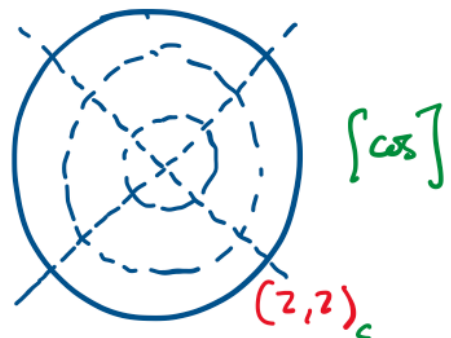
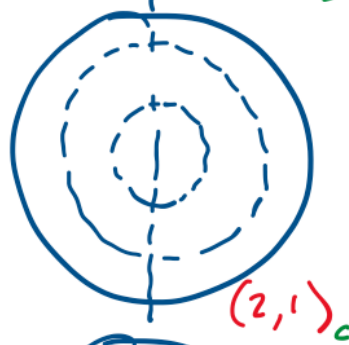
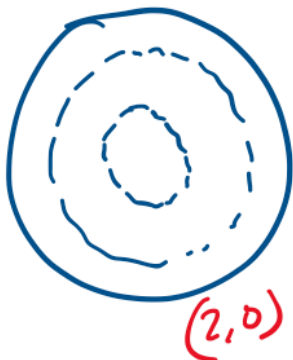
1



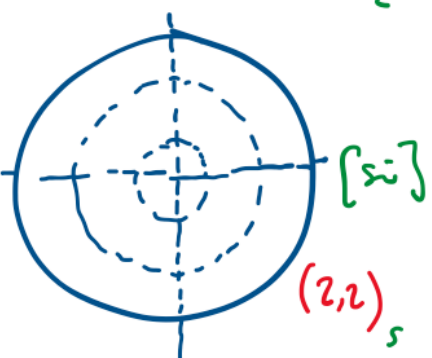
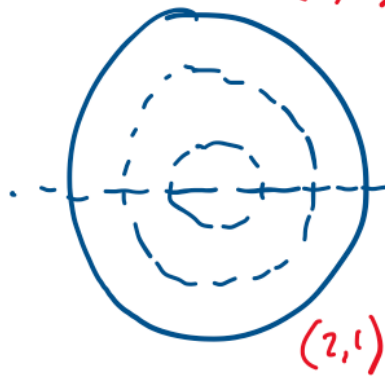
1



2



2



(c) note $k^2 = \rho \frac{\omega^2}{\rho}$, i.e. $\omega = k \sqrt{\rho/\rho}$

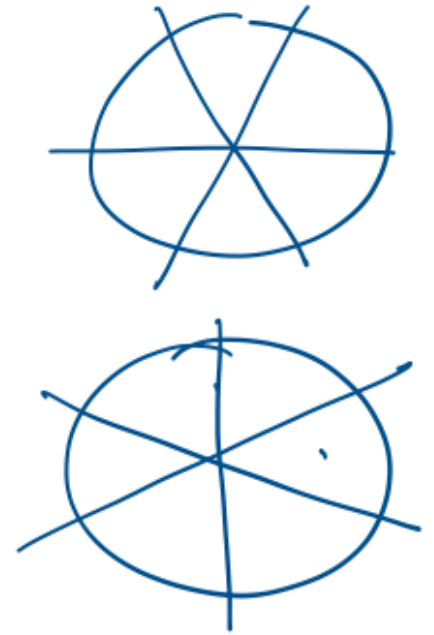
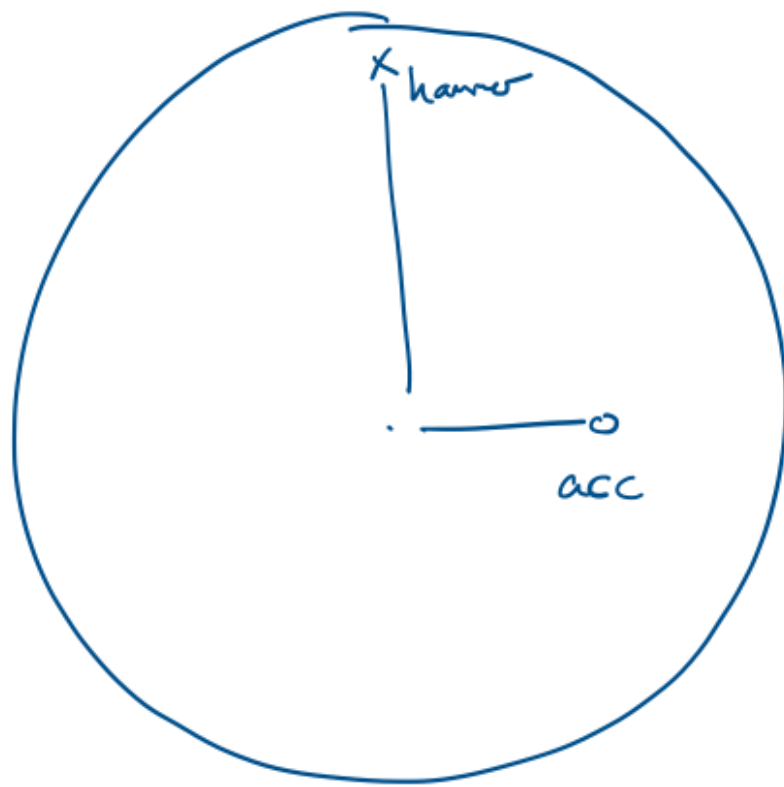
$$= \frac{1}{a} \cdot ka \cdot \sqrt{\rho/\rho}$$

$$= 100 \cdot ka //$$

mode	ka	$\omega = 100ka \text{ rad s}^{-1}$
(0,0)	2.4	240
(0, ①)	3.83	383 — ^{see} x(d)
(0, 2)	5.14	514
(①, 0)	5.52	552 — x(d)
(0, ③)	6.38	638 — x(d)
(1, ①)	7.02	702 — x(d)

//

(d)



Accelerometer splits all doublet nodes, and orients node shapes to be symmetric/antisymmetric about it.

Positioning of acc & kammer $\Rightarrow n=1$ & $n=3$
nodes not visible: $\ominus \oplus$, & $\otimes \otimes$.

Also on $n=0$ nodal circle, so $(1,0)$ not visible,

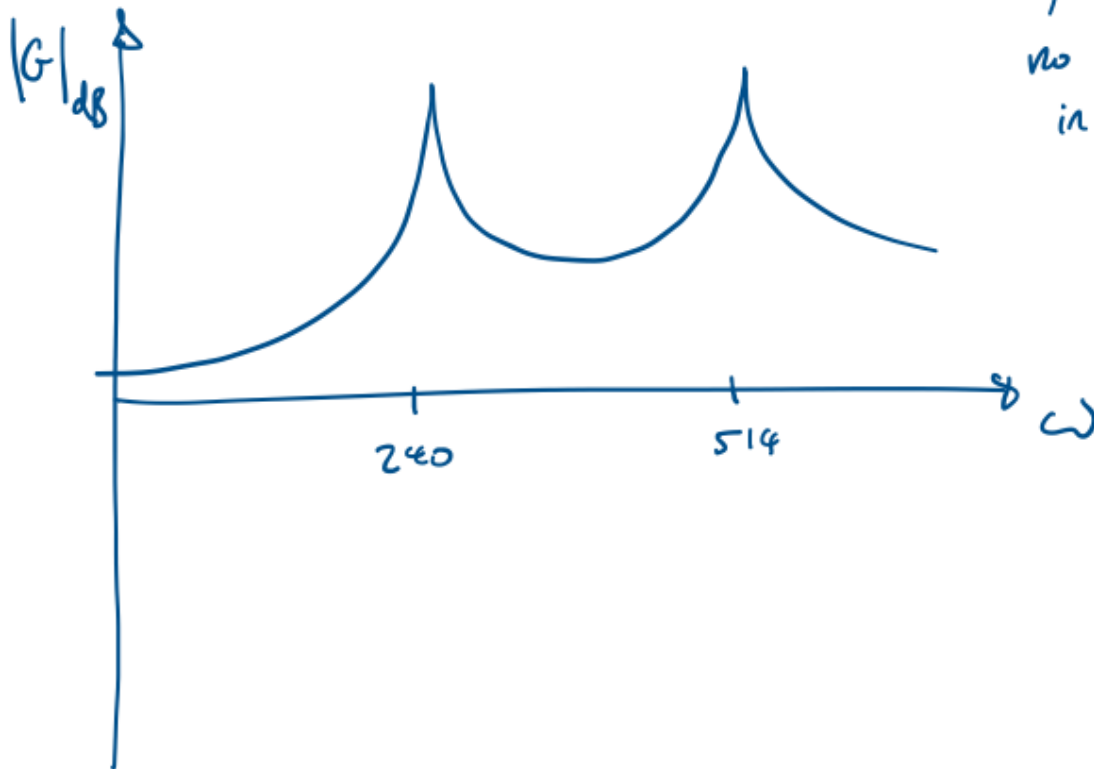
as $0.435 = 2.4 / 5.52$.

Note for $(1,2)$, nodal circle is at $0.654a$.

Remaining modes:

$(0,0)$	\odot	$++ = +$	ω
			240
$(0,2)$	\otimes	$+ - = -$	ω
			514

↑
no antiresonance
in between



e) all modes with nodal diameters ($n \geq 1$):

- one mode unchanged
- one will decrease but not beyond next mode 'down'.

all other modes ($n=0$):

- frequency will decrease but not beyond next mode 'down'.

(f) ($n \geq 1$):

- one mode unchanged
- one mode increase but not beyond next mode 'up'.

($n=0$):

- frequency will increase but not beyond next mode 'up'.

Final frequencies will be same as (e) but (e) will have additional low frequency mode.

Q4

(a)

$$R = \frac{V}{\tilde{T}} \begin{array}{l} \longrightarrow \text{depends on complex moduli.} \\ \longrightarrow \text{unchanged} \end{array}$$

$$\omega^2 \approx \frac{E(1+i\gamma_E) \int \left(\frac{\partial^2 y}{\partial x^2}\right)^2 dx}{\tilde{T}}$$

$$= \omega_n^2 (1+i\gamma_E)$$

$$\omega \approx \omega_n \left(1 + \frac{1}{2}i\gamma_E\right)$$

free response $y \propto e^{i\omega_n t} \cdot e^{-\frac{1}{2}\gamma_E \omega_n t}$

cf: $e^{i\omega_n t} \cdot e^{-\zeta \omega_n t}$

$$\Rightarrow \zeta = \frac{1}{2}\gamma_E$$

$$Q = \frac{1}{2\zeta} = \frac{1}{\gamma_E}$$

- (i) Carbon fibre: $\eta_E \approx 0.002$, $Q \approx 500$ ✓
- (ii) Titanium: $\eta_E \approx 0.0005$, $Q \approx 2000$ ✓
- (iii) Wood: $\eta_E \approx 0.01$, $Q \approx 100$ ✓✓

$$(c) \quad EI = E_1 \left(\frac{h_1^3}{6} + \frac{h_1(h_1+h_2)^2 g}{1+2g} \right) + E_2 \left(\frac{h_2^3}{12} - \frac{h_2^2(h_1+h_2)}{12(1+2g)} \right)$$

$$h_1 = 0.0005$$

$$h_2 = 0.01$$

$$E_1 = 100 \times 10^9 \times (1 + i\eta_1) \quad , \quad \eta_1 = 0.002 \quad \text{CFRP}$$

$$E_2 = 10 \times 10^9 \times (1 + i\eta_2) \quad , \quad \eta_2 = 0.01 \quad \text{WOOD}$$

$$G_2 = E_2/3 \times (1 + i\eta_g) \quad , \quad \eta_g = 0.1 \quad \text{WOOD SHEAR.}$$

Substitute values into EI:

$$EI = 3589 + 14.1j$$

$$Q_{\text{eff}} \approx 3589/14.1 \approx 255 \quad \checkmark$$

Values consistent with loss factors chosen for wood & CFRP accepted.

$$(d) \quad g \rightarrow g(1 + i\tau_c)$$

$$\text{so} \quad \frac{1}{1+2g} = \frac{1}{1+2g(1+i\tau_c)}$$
$$= \frac{1/1+2g}{1 + i\tau_c/(1+2g)}$$

$$\approx \frac{1}{1+2g} \left(1 - \frac{i\tau_c}{1+2g} \right)$$

$$EI = EI(g_0 + i\Delta)$$

EI is a function of g

$$g \rightarrow g_0 + i\Delta$$

then use Taylor approximation.

$$\approx EI(g_0) + i\Delta \frac{\partial EI}{\partial g}$$

$$\text{Im}(EI) \approx \Re \left[\frac{\partial EI}{\partial g} \cdot \Delta \right] \quad \& \quad \Delta = \tau_c g.$$

$$\frac{\partial EI}{\partial g} = E_1 \frac{h_1(h_1+h_2)^2 [(1+2g) - 2g]}{(1+2g)^2} + E_2 \frac{2h_2^2(h_1+h_2)}{12(1+2g)^2}$$

$$= E_1 \frac{h_1(h_1+h_2)^2}{(1+2g)^2} + E_2 \frac{2h_2^2(h_1+h_2)}{12(1+2g)^2}$$

$$= \frac{12E_1 h_1(h_1+h_2)^2 + E_2 \cdot 2h_2^2(h_1+h_2)}{(1+2g)^2}$$

so $im(EI) \propto \frac{g}{(1+2g)^2}$.

max when $\frac{\partial im(EI)}{\partial g} = 0$.

$$\frac{\partial \left(\frac{g}{(1+2g)^2} \right)}{\partial g} = \frac{(1+2g)^2 - g \cdot 4(1+2g)}{(1+2g)^4} = 0 \quad \text{at max.}$$

$$\Rightarrow 4g^2 + \cancel{4g} + 1 - \cancel{4g} - 8g^2 = 0.$$

$$4g^2 = 1$$

$$g = \frac{1}{2}.$$

$$G_2 = \frac{1}{2} E_3 h_3 h_2 \rho^2$$

$$= 2.47 \times 10^6 \text{ Pa} //$$

$$Q_{\text{eff}} \approx 20 //$$

Note: we have not calculated max possible Q_{eff} , just Q when $\text{im}(EI)$ is maximised.

(e) Performance of CFRP-wood-CFRP is between wood & CFRP individually. Not too surprising, although with different geometry it can be lighter damping than CFRP alone.

Optimised value for G_2 shows high damping can be achieved but requires rather specific material properties.

ASSESSOR'S COMMENTS, MODULE 4C6

Q1

This was a popular question, being attempted by 21 candidates. Parts (a) to (c) were generally answered well. Most candidates correctly formulated the first order equations of motion in (d). Part (e) was more variable, with several candidates unclear on the physical interpretation of complex modes, and the table in part (e)(iv) was not always complete. No candidates noticed that damping between all floors in (e)(v) could lead to proportional damping but many made sensible comments, gaining some of the marks available here.

Q2

This was the most popular question, being attempted by 24 candidates. A surprising number did not accurately derive the ODE's for R and F using separation of variables in part (a). Sketches of the modes in part (b) were generally good, though many missed the doublet pairs of modes. The mode sequence was listed accurately by most in (c), and marks were awarded whether the doublet pairs were counted separately or not, as this was ambiguous in the question (marks were carried through to part (d) when working was correct). The transfer function sketches showed considerable variation, depending on which modes were identified as being visible in the measurement. Parts (e) and (f) were generally sound, but few noticed that the frequencies would end up the same for both parts.

Q3

This question was attempted by 15 candidates and was generally well done, with the majority of candidates gaining marks in all parts. The quality of sketching of the response functions varied considerably, and many lost marks by failing to highlight the important features asked for.

Q4

This question was attempted by 15 candidates and was, without exception, done poorly. Most demonstrated some understanding of Rayleigh's principle and the correspondence principle in part (a) but none formally derived the Q-factor in terms of loss factor. Parts (b) and (c) were done particularly poorly, with candidates getting lost in the complex algebra.

T Butlin
J P Talbot